

## Cellular Automaton Models for Reaction Diffusion Equations

Jörg R. Weimar and Layne T. Watson  
Department of Computer Science  
Virginia Polytechnic Institute  
and State University  
Blacksburg, VA 24061-0106

John J. Tyson  
Department of Biology  
Virginia Polytechnic Institute  
and State University  
Blacksburg, VA 24061-0406

### Abstract

*This paper introduces a new cellular automaton model for reaction diffusion equations with improved treatments of (1) diffusion and wave propagation, and (2) slow dynamics of the recovery variable. The automaton is both computationally efficient on a distributed memory multiprocessor and faithful to the underlying partial differential equations.*

### 1 Introduction

Excitable media support undamped traveling waves of excitation, such as waves of membrane depolarization in nerve axons and waves of star formation in galactic dust clouds. Traditionally, excitable media have been modeled either by partial differential equations or by cellular automata.

Some simple (two-variable) reaction diffusion partial differential equation models of the form

$$(1) \quad \begin{aligned} \frac{\partial \hat{u}}{\partial t} &= \epsilon \nabla^2 \hat{u} + \frac{1}{\epsilon} f(\hat{u}, \hat{v}), \\ \frac{\partial \hat{v}}{\partial t} &= g(\hat{u}, \hat{v}), \end{aligned}$$

have become popular representations of excitable media, e.g., the Oregonator model of the Belousov-Zhabotinskii reaction [2], and the FitzHugh-Nagumo [1] model of neuromuscular membranes. The earliest model of excitable media was a cellular automaton introduced by Wiener and Rosenblueth [5] in 1946, and the cellular automaton approach was pursued later by others. These “first generation models” featured nearest neighbor connections and only a few possible states per cell. Although they exhibited wave propagation, they failed in several crucial aspects: curvature effects, dispersion relations, and spatial isotropy. These three shortcomings have been addressed in “second generation” models by Gerhardt, Schuster and Tyson [2] and others. Their automaton models curvature effects and dispersion, but still suffers somewhat from directional anisotropy. Markus and Hess [3] addressed the problem of directional anisotropy by introducing semi-random grids, which achieved good isotropy at the cost of high computational complexity.

This paper introduces a “third generation” automaton that combines the strengths and avoids the weaknesses of these earlier versions. Furthermore, the cellular automaton (CA) rules are closely related to the underlying reaction diffusion equations (1).

### 2 Description of new mask

Gerhardt, Schuster and Tyson used a square mask because the operation of counting the number of excited neighbors can be done in a time independent of the size of the mask. This property is very desirable, especially for big masks. The basic idea is to construct a square mask as the convolution of a vertical strip and a horizontal strip. The sum within a strip is calculated by a scanning operation.

Another mask (a diamond mask) can be constructed as the convolution of two diagonal strips. The new mask is calculated as the convolution of a square mask and a diamond mask. The results of its application to a data array can be calculated with 8 addition operations per cell, independent of the size of the mask. The examples here use a square mask of radius 3 and a diamond mask that is constructed from diagonal strips of length 5 (radius 2). The “combination” mask closely resembles a Gaussian mask.

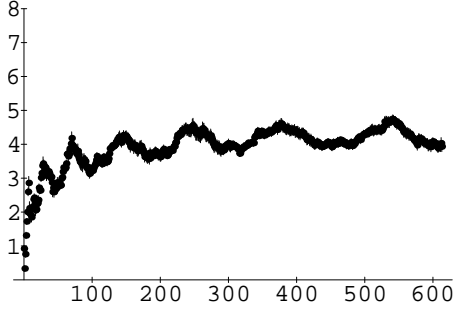
A crucial test for this mask is the curvature relationship,  $N = c + DK$ , which is tested by simulations of waves with different curvatures. The mask exhibits a linear relationship with an effective diffusion coefficient of 4, almost independent of the threshold at which the speed of propagation is determined. Figure 1 summarizes the simulation results.

### 3 Construction of cellular automaton rules from the PDE model

In the PDE model (1),  $\epsilon$  is a small (positive) parameter representing the time scales for changes in  $\hat{u}$  (the fast variable) and  $\hat{v}$  (the slow variable). The smallness of  $\epsilon$  makes numerical solution of (1) difficult, but it can be exploited by singular perturbation theory to show that

1. traveling wave solutions are possible for these systems;

D(k) : diffusion coefficient vs. threshold.



c(k) : speed vs. threshold.

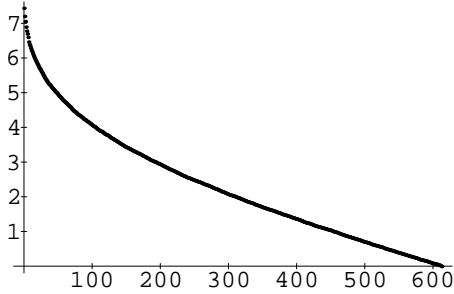


Figure 1.

2. away from the wavefronts and wavebacks  $\hat{u}$  changes very little, so that  $f(\hat{u}, \hat{v}) \approx 0$ ;
3. within the wavefronts and wavebacks,  $\hat{v}$  changes very little, since  $\hat{v}$  is a slow variable.

Solving the equation  $f(\hat{u}, \hat{v}) = 0$  for  $\hat{u}$  gives three solution branches,

$$\hat{u} = h_-(\hat{v}), \quad \hat{u} = h_0(\hat{v}), \quad \hat{u} = h_+(\hat{v}),$$

two of which ( $h_-(\hat{v})$  and  $h_+(\hat{v})$ ) are stable. These two branches determine the value of  $\hat{u}$  in the regions between wavefronts and wavebacks.

The value of  $\hat{v}$  is limited by  $\hat{v}_{\min} \leq \hat{v} \leq \hat{v}_{\max}$ , where  $\hat{v}_{\min}$  is the value of  $\hat{v}$  at the resting state, i.e., the stable solution of  $g(\hat{u}, \hat{v}) = 0$  and  $f(\hat{u}, \hat{v}) = 0$ . Likewise,  $\hat{v}_{\max}$  is the value of  $\hat{v}$  at which  $h_0(\hat{v}) = h_+(\hat{v})$ . At this value of  $\hat{v}$ ,  $h_+(\hat{v})$  is not stable. At  $\hat{v} = \hat{v}_{\max}$ , a waveback occurs as a jump from  $\hat{u} = h_+(\hat{v})$  to  $\hat{u} = h_-(\hat{v})$ .

In order to model a PDE of this sort, introduce two variables  $u, v$  in the cellular automaton:

$$u = \begin{cases} 0 & \text{if } \hat{u} = h_-(\hat{v}), \text{ (recovering state)} \\ 1 & \text{if } \hat{u} = h_+(\hat{v}), \text{ (excited state)} \end{cases}$$

and

$$v = L(\hat{v}) := \frac{\hat{v} - \hat{v}_{\min}}{\hat{v}_{\max} - \hat{v}_{\min}} v_{\max\text{aut}}.$$

Diffusion of the variable  $u$  and the excitation jump at the wavefront are simulated by using a big mask

to count the number of excited cells in the neighborhood and applying a threshold function to the resulting (weighted) count  $Sum$ . This threshold function is selected such that the correct wave speed is obtained for all values of  $\hat{v}$ . Calculate from the PDE the planar wave speed  $c = c_2(\hat{v})$  of an isolated front propagating into medium with recovery value  $\hat{v}$ . From the mask, a simulation gives the function  $c_1(k)$ , the planar wave speed as a function of the threshold (averaged over all directions). These two speeds should be equal (in their respective time and space scales) for all values of  $\hat{v}$ . Therefore

$$k(v) = c_1^{-1}(\alpha c_2(L^{-1}(v))).$$

Here  $L^{-1}$  is an affine transformation from the automaton variable  $v$  into the PDE variable  $\hat{v}$  and  $\alpha$  transforms the units of measurement for wave speeds.

So a rule for updating  $u$  in the automaton is:

$$\begin{aligned} Sum &:= Mask * u^t ; \\ \text{if } Sum > k(v) &\text{ then } u^{t+1} = 1 \\ &\text{else } u^{t+1} = 0; \end{aligned}$$

where the superscript refers to the time step  $t$  and ‘\*’ denotes convolution.

The update function for  $v$  is obtained directly from the PDE for  $\hat{v}$ :

$$\frac{\partial \hat{v}}{\partial t} = \begin{cases} g(h_+(\hat{v}), \hat{v}) & \text{if } u = 1; \\ g(h_-(\hat{v}), \hat{v}) & \text{if } u = 0. \end{cases}$$

The rule for updating  $v$  in the automaton is:

$$\begin{aligned} \text{if } v^t = v_{\max\text{aut}} &\text{ then} \\ &u^{t+1} = 0; v^{t+1} = v_{\max\text{aut}} \\ \text{else if } u^t = 0 &\text{ then} \\ &v^{t+1} = \max\{0, v^t + \lfloor L' g_-(v) \Delta t \rfloor\} \\ \text{else if } u^t = 1 &\text{ then} \\ &v^{t+1} = \min\{v_{\max\text{aut}}, v^t + \lceil L' g_+(v) \Delta t \rceil\}, \end{aligned}$$

where  $L' = dL/d\hat{v} = v_{\max\text{aut}}/(\hat{v}_{\max} - \hat{v}_{\min})$ ,  $g_{\pm} = g(h_{\pm}(\hat{v}), \hat{v})$  with  $\hat{v} = L^{-1}(v)$ , and  $\Delta t$  is the length of one CA time step measured in PDE time units.

If  $v_{\max\text{aut}}$  is big, the error introduced by the discretization of  $\hat{v}$  (the  $\lfloor \cdot \rfloor$  and  $\lceil \cdot \rceil$  operations) is small.

## 4 Spiral wave simulation

To complete the description of a CA model, the functions  $f(\hat{u}, \hat{v})$  and  $g(\hat{u}, \hat{v})$  in (1) must be specified. The Oregonator model is chosen:

$$\begin{aligned} f(\hat{u}, \hat{v}) &= \hat{u}(1 - \hat{u}) - \hat{f}\hat{v}(\hat{u} - q)/(\hat{u} + q), \\ g(\hat{u}, \hat{v}) &= \hat{u} - \hat{v}, \end{aligned}$$

with  $\hat{f} = 3$  and  $q = 0.002$ . The values of the CA space constant and time step,  $\Delta x$  and  $\Delta t$ , measured in PDE units, are obtained by identifying (1) diffusion coefficients and (2) solitary plane wave speeds in the PDE and CA models. With all this machinery

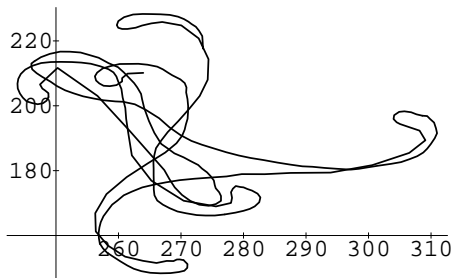


Figure 2.

in place, a rotating spiral wave was calculated on a  $400 \times 400$  grid of cells. A snapshot of a spiral is shown in Figure 3, where the region of excitation is outlined in white and the greylevels indicate the value of the recovery variable  $v$ . Numerous other snapshots of a spiral are shown in [4]. This CA simulation of the spiral wave shows many features that appear in simulations of the Oregonator PDEs by standard numerical methods, even down to the “meandering” of the tip of the spiral (Figure 2 shows the motion of the tip of the spiral for  $t = 3900$  to  $t = 4200$ ).

## 5 Parallel implementation

Parallel implementation on a ring-connected multicomputer is straightforward: for  $p$  processors, the simulation domain is split into  $p$  strips of equal width. Each processor stores this strip plus two overlap areas each with a width equal to the radius of the mask. At the end of each cellular automaton step, which is carried out exactly as in the sequential implementation, the information in the overlap areas is updated by messages between neighboring processors. This scheme is efficient as long as the width of each strip is larger than the size of the mask used. Some speed examples on the Intel iPSC/860 hypercube with 128 processors are listed in Table 1. Here  $N_{int}$  refers to the number of cells in the x-direction assigned to each processor. In the y-direction there are 700 cells. Thus the total amount of work is proportional to the number of processors. These measurements are taken without control over the load of the host processor, which is the bottleneck for small  $N_{int}$ . Also, each reported run time is the result of averaging 3 or 4 runs with 200 steps each. Factors influencing the performance are (i) the speed of the host and (ii) the cache hit ratio on the i860 processors. It can be seen that the overhead for higher degrees of parallelism is negligible (the execution time is independent of the number of processors if the problem size is proportional to the number of processors as

Table 1: Times in  $\mu sec$  for one cell-update.

$p$	$N_{int} = 15$	$N_{int} = 25$	$N_{int} = 100$	$N_{int} = 400$
1	14.33	11.95	6.56	7.83
4	12.39	8.76	6.85	7.83
16	12.14	9.33	6.85	7.83
64	12.83	9.62	6.85	7.83
128	12.75	9.91	-	-

in the columns of Table 1). In other words, this application belongs to the applications ideally suited even for distributed memory parallel machines.

## 6 Conclusion

A new way to construct a cellular automaton for simulating excitable media has been presented. The construction is based on singular perturbation analysis of the partial differential equation models for excitable media, and it shows the close relationship between the cellular automaton and the PDEs. It is not necessary to use the simulation results for tuning parameters, since all aspects of the automaton rule are derived from the PDE model. This approach is applicable to all PDE models that can be expressed in the form of (1), with a small parameter  $0 < \epsilon \ll 1$ . Since simulations of this automaton are computationally inexpensive compared to numerically solving the PDE, three dimensional calculations become more feasible.

## References

- [1] R. FitzHugh, “Impulse and physiological states in models of nerve membrane,” *Biophysics J.*, Vol. 1, pp. 445–466, 1961.
- [2] M. Gerhardt, H. Schuster, and J. J. Tyson, “A cellular automaton model of excitable media including curvature and dispersion II. Curvature, dispersion, rotating waves and meandering waves,” *Phys. D*, Vol. 46, pp. 392–415, 1990.
- [3] M. Markus and B. Hess, “Isotropic cellular automaton for modelling excitable media,” *Nature*, Vol. 347, pp. 56–58, 1990.
- [4] J. R. Weimar, “Cellular automata models for excitable media,” MS Thesis, Dept. of Computer Science, VPI & SU, Blacksburg, VA, 1991.
- [5] N. Wiener and A. Rosenblueth, “The mathematical formulation of the problem of conduction of impulses in a network of connected excitable elements, specifically in cardiac muscle,” *Arch. Inst. Cardiol. de Mexico*, Vol. 16, pp. 205–265, 1946.

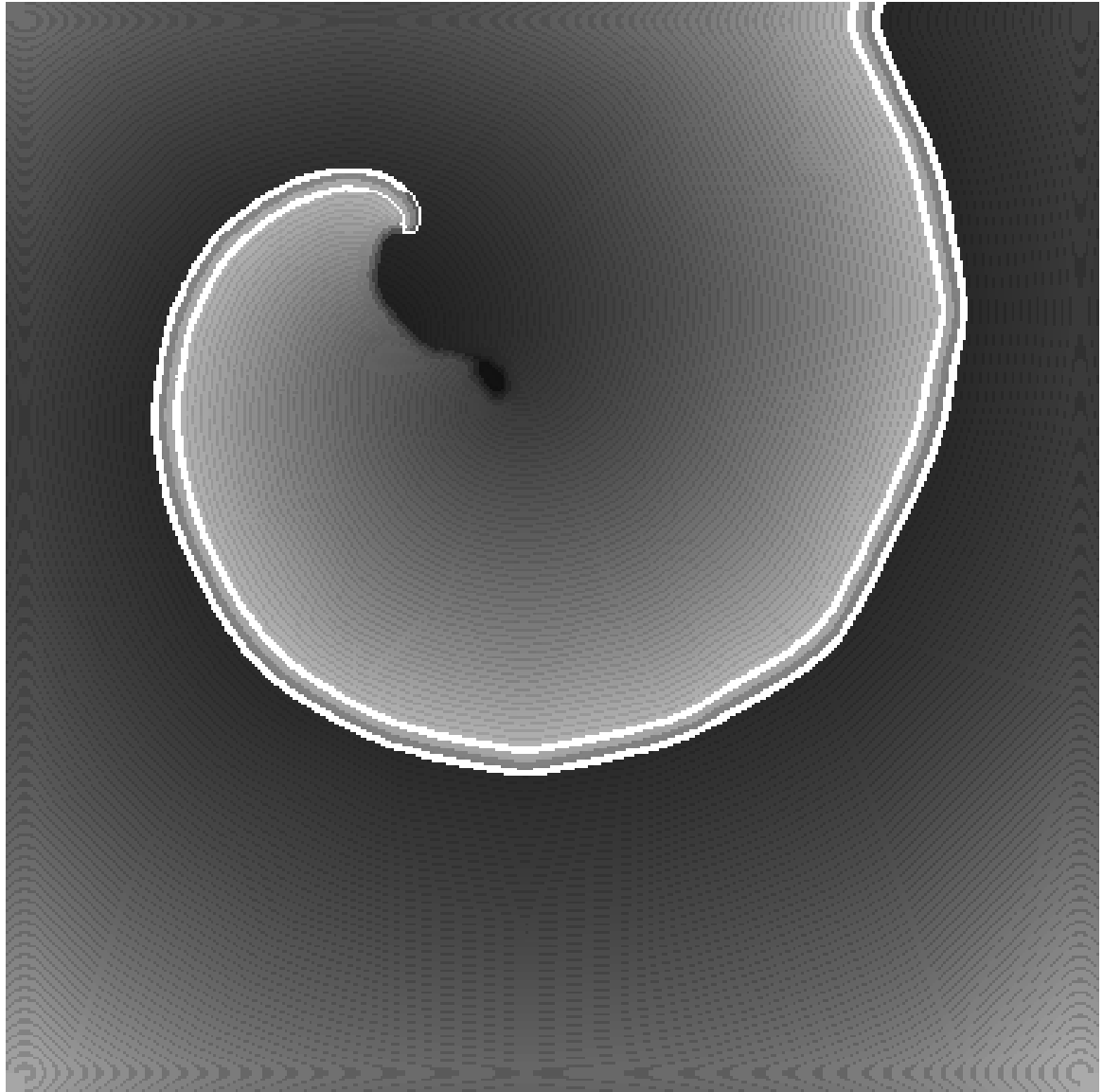


Figure 3. Spiral wave calculated by the automaton, showing  $v$ .